JIRBDAI

Journal of Institutional Research, Big Data Analytics and Innovation

Integrated Petrophysical Evaluation of Reservoir Quality and Hydrocarbon Potential Using Thickness-Weighted Metrics from Well Logs in the Niger Delta

Francis Omonefe[1]*, Edeye Ejaita[2], Arekumo ThankGod[3]

[1*]Department of Geology, Federal University Otuoke, Bayelsa state, Nigeria

[2]Department of Physics, Niger Delta University, Wilberforce Island, Amassoma, Bayelsa state, Nigeria.

[3]Department of Physics, Federal University Otuoke, Bayelsa state, Nigeria.

*Corresponding Author: francisoo@fuotuoke.edu.ng

ABSTRACT

Reservoir ranking in heterogeneous deltaic successions requires consideration of both rock properties and net reservoir thickness. This study evaluates five intervals in each of two Niger Delta wells using gamma-ray, resistivity, neutron-porosity and density logs, complemented by net-to-gross ratio (N/G), porosity-thickness (ΦH) and hydrocarbon-filled porosity-thickness ($\Phi S_h H$). These products are established volumetric proxies; the contribution here is their explicit comparison with conventional interval-average measures across ten interpreted zones. The most favourable intervals were Well 1 Zones 1, 3 and 5 and Well 2 Zones 1, 3 and 5. Well 2 Zone 5 had the highest reported ΦH (43.81 ft) and $\Phi S_h H$ (41.39 ft), with porosity 39.4%, water saturation 5.5% and N/G 0.923. In contrast, Well 2 Zones 2 and 4 had porosities of 41.8% and 42.9% but low N/G (0.019 and 0.010), illustrating the limitations of porosity-only ranking. Reported thickness-weighted values are consistent with zone-average inputs to the displayed precision. This log-based screening does not establish permeability, producibility, recoverable reserves or fluid type without independent evidence. Further calibration of Archie parameters, net-pay cutoffs and log interpretations is required for reproducibility and confirmation. The novelty of this study lies not in the development of new thickness-weighted equations, which are established in reservoir evaluation, but in their systematic application as complementary quantitative ranking indicators alongside conventional petrophysical parameters to distinguish between highly porous but volumetrically limited intervals and reservoirs with substantial hydrocarbon-filled storage capacity in the investigated Niger Delta wells.

KEYWORDS: Petrophysical Evaluation; Thickness-weighted Metrics; LAS Well Logs; Hydrocarbon Pore Volume; Reservoir Characterization; Niger Delta.

I. INTRODUCTION

The accurate characterization of subsurface reservoirs is fundamental to hydrocarbon exploration and production (Volokitin & Khabarov, 2010). In mature hydrocarbon provinces such as the Niger Delta, the increasing complexity of reservoir architecture necessitates the adoption of advanced petrophysical techniques capable of capturing both vertical and lateral heterogeneity (Deabl et al., 2021). Traditional reservoir evaluation methods rely heavily on parameters such as porosity, permeability, and fluid saturation; however, these parameters, when considered independently, often fail to adequately represent the integrated storage and flow capacity of the reservoir system

Volume 2, Issue 3, 2026

https://doi.org/10.5281/zenodo.23624877

(Sharif, 2024). The challenge is particularly pronounced in deltaic systems, where rapid facies transitions, interbedding of sands and shales, and structural compartmentalization introduce significant variability in reservoir properties over short spatial scales (Chukwuemeka et al., 2025). As highlighted in previous studies, the Niger Delta Basin is characterized by stacked sedimentary sequences formed through progradation processes, resulting in complex stratigraphic and structural traps that control hydrocarbon accumulation (Kuye & Hampson, 2023). Fluid saturation, particularly the ratio of hydrocarbons to water within the pore spaces, is another critical factor in petrophysical evaluation (Omoja et al., 2026). However, unconventional reservoirs often exhibit mixed wettability, where both oil and water are present, complicating the use of conventional resistivity logs to estimate fluid saturation accurately (Knackstedt et al., 2013). In such cases, advanced techniques like nuclear magnetic resonance (NMR) logging or dielectric logging may be employed to improve the accuracy of saturation estimates (Herlinger, 2019; Bassey, 2015). Despite advancements in petrophysical techniques, several challenges remain in the evaluation of unconventional reservoirs (Sarhan, 2025). One of the primary challenges is the accurate measurement of porosity and permeability in tight formations (Shabani et al., 2022; Osman et al., 2025). The presence of micro-porosity, combined with the low permeability of the reservoir rock, makes it difficult to obtain representative measurements using traditional well logging tools (Ejaita & Omonefe, 2026). Core analysis, while more accurate, is time-consuming and expensive, and may not always be feasible for large-scale reservoir studies (Zhang et al., 2020).

Another challenge is the accurate determination of fluid saturation in unconventional reservoirs (Nabawy, 2025). Mixed wettability, where both oil and water are present in the pore spaces, can complicate the interpretation of resistivity logs (Sneider et al., 1978). Advanced techniques such as NMR or dielectric logging can improve the accuracy of saturation measurements, but these methods are also more expensive and require specialized expertise (Nikolaev & Kazak, 2019). The present study integrates log-derived porosity, saturation and net thickness to rank ten interpreted intervals in two Niger Delta wells. Porosity-thickness and hydrocarbon-filled porosity-thickness are established quantities. The specific contribution is a transparent zone-by-zone comparison showing how interval thickness changes ranking relative to porosity alone, particularly where high-porosity intervals contain very little net sand. As the evaluation is limited to two wells and lacks core or flow-test validation, its findings are screening-level indications of potential storage rather than demonstrated reservoir performance. Figure 1 identifies the relative locations of Wells 01 and 02 within the studied portion of the Niger Delta. The map provides geographical context but, in the absence of structural-depth mapping and seismic ties, cannot by itself demonstrate lateral reservoir connectivity. The Niger Delta comprises a thick Cenozoic clastic succession accumulated along the Gulf of Guinea continental margin (Reijers et al., 1997; Doust & Omatsola, 1989).

Volume 2, Issue 3, 2026
https://doi.org/10.5281/zenodo.23624877

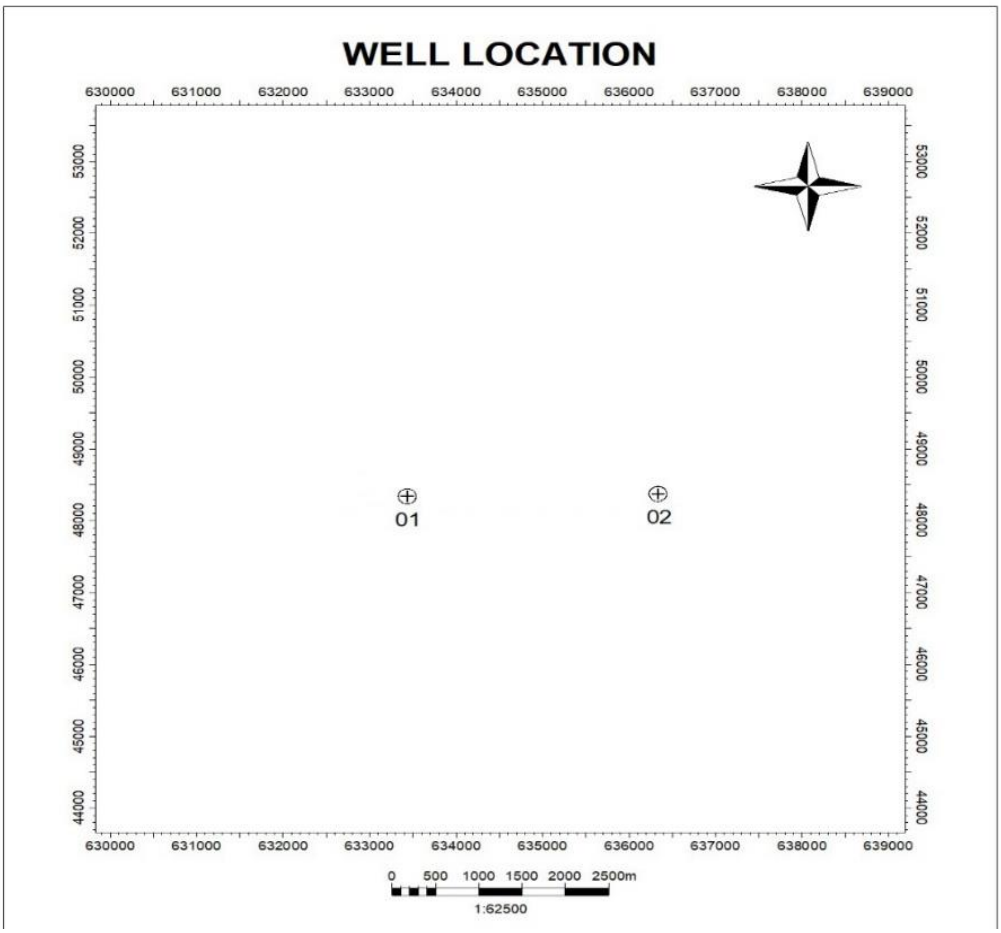


Figure 1: Map of the Field

The lithology of the Niger Delta is characterized by a complex arrangement of sandstones, shales, and siltstones deposited in varying depositional environments, which include fluvial, deltaic, and marine settings (Figure 2) (Momta et al., 2015). The lithological sequence is stratified into three primary formations that define the geological architecture of the Niger Delta Basin: The Benin Formation is the uppermost layer and is composed of continental deposits from fluvial processes (Olabode & Mohammed, 2016). It primarily consists of unconsolidated sandstones interbedded with clay, representing a depositional environment dominated by rivers and floodplains. The Benin Formation ranges from the Oligocene to the present day and extends to depths of approximately 2000 meters (Reijers, 2011). Its sands are often non-hydrocarbon-bearing, but they provide structural support for the overlying formations (Olabode, 2006).

Volume 2, Issue 3, 2026
https://doi.org/10.5281/zenodo.23624877

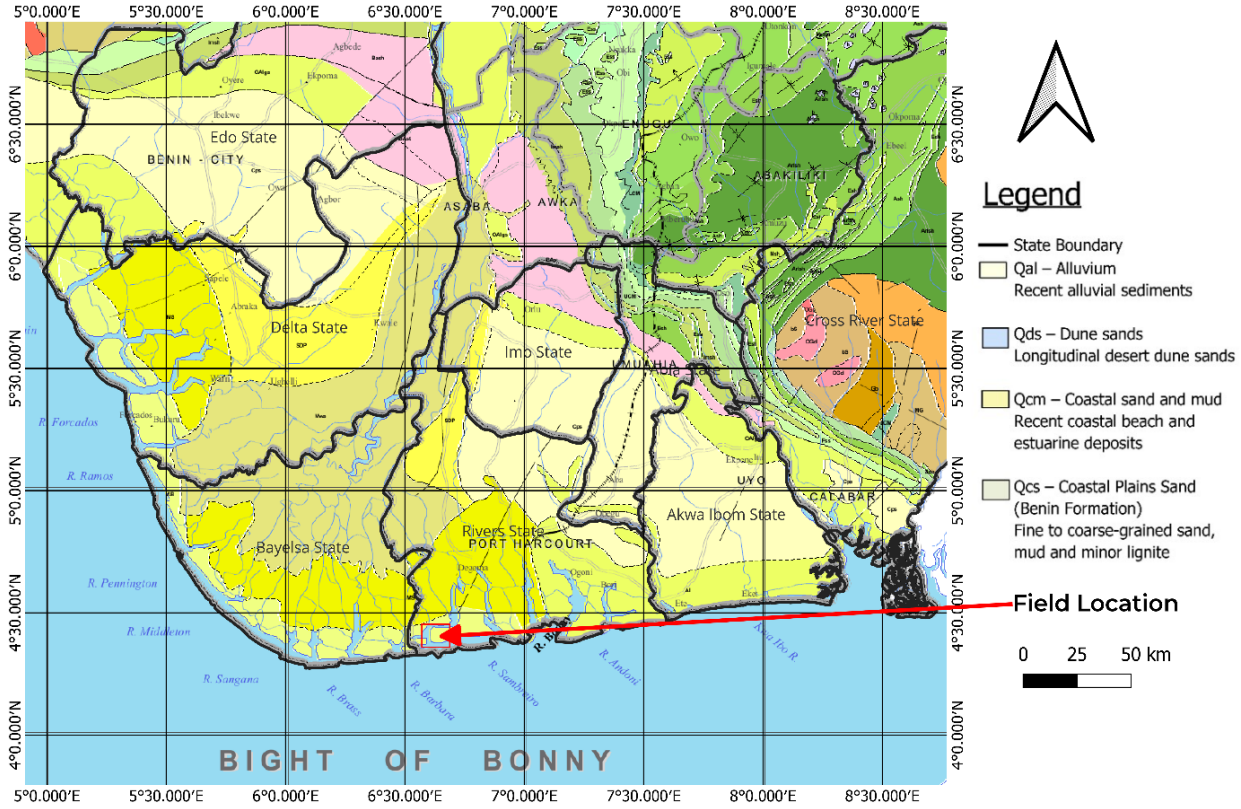


Figure 2: Litho-Structural Map of the Niger Delta

The Agbada Formation is the primary reservoir-bearing unit of the Niger Delta. It consists of an alternating sequence of sandstones and shales, deposited in deltaic and shallow marine environments (Overare et al., 2024; Plumley, 1992). The sandstones in the Agbada Formation serve as the primary hydrocarbon reservoirs, while the shales function as both source and cap rocks, trapping hydrocarbons within the formation (Reijers, 2011). This formation's thickness can exceed 3,500 meters, and it is the most economically significant due to its oil and gas-bearing zones. The Agbada Formation dates from the Eocene to the present, reflecting millions of years of sedimentation driven by the Niger River (Reijers et al., 1997). The Akata Formation is the deepest lithological unit of the Niger Delta and is composed primarily of marine shales. These shales were deposited in deep marine settings during the early stages of the delta's formation and are thought to act as the main hydrocarbon source rock for the overlying reservoirs (Haack et al., 2000). The Akata Formation ranges from the Paleocene to the present and can reach thicknesses of more than 6,000 meters in some areas. Its organic-rich shales were deposited during periods of low oxygen levels in marine waters, leading to the preservation of organic matter essential for hydrocarbon generation (Reijers et al., 1997). The Niger Delta is an archetypal example of a wave-dominated deltaic system, where sediment deposition is influenced by fluvial input, wave action, and longshore currents (Omonefe et al., 2020). The Niger River, one of Africa's largest, has been the primary agent of sediment transport, depositing vast amounts of detritus that have accumulated in the delta over millions of years. These depositional processes have created a diverse array of

Volume 2, Issue 3, 2026
https://doi.org/10.5281/zenodo.23624877

environments, each contributing to the region's complex stratigraphy and petroleum system (Ejaita & Omonefe, 2026).

The delta is dissected by a complex network of distributary channels, forming classic fluvial-deltaic systems. These systems deposit coarse-grained sandstones in proximal regions, gradually transitioning to finer sediments such as shales and siltstones toward the distal portions of the delta. These fluvial deposits form the core of the reservoir rock within the Agbada Formation (Huang et al., 2025). During periods of low sea level, the river's energy deposited larger, coarser sediments, while higher sea levels allowed for more fine-grained deposition (Kiss et al., 2022). The distal portions of the Niger Delta extend offshore into the shallow marine environment, where finer sediments, such as silts and clays, are deposited by longshore currents and tidal processes. The transition from deltaic to marine deposition is reflected in the lithology of the Agbada and Akata Formations, with alternating layers of sandstone and shale indicating fluctuating sea levels and changing depositional environments (Allen, 1970). These transitions are key in understanding the vertical and lateral facies changes within the reservoir (Ezeh et al., 2016). Over geologic time, the Niger Delta has grown seaward through a process called progradation, where sediments build outward from the continent toward the ocean. This process has created a stacked sequence of sedimentary deposits, with older layers buried beneath younger sediments (Konyukhov, 2008). Each depositional cycle represents a phase of delta growth, influenced by factors such as sea-level change, sediment supply, and tectonic activity. These progradational sequences are responsible for the multi-layered hydrocarbon reservoirs found in the Niger Delta (Bello et al., 2026).

The formation of the Niger Delta is intricately linked to the tectonic evolution of the West African margin. The development of the delta began in the late Cretaceous and has continued through to the present, driven by the interplay of tectonics, sediment supply, and sea-level changes (Bonne, 2014). The Niger Delta Basin formed as part of a passive continental margin following the separation of the African and South American plates during the early Cretaceous (Stoneley, 1966). As the Atlantic Ocean opened, the crust along the West African margin began to subside, creating accommodation space for sediment deposition. This subsidence, combined with sediment influx from the Niger River, facilitated the accumulation of thick sedimentary sequences (Doust & Omatsola, 1989). The Niger River, along with its numerous tributaries, has been the primary source of sediment for the delta (Spina et al., 2025). Over millions of years, the river has transported vast amounts of sediment from the interior of the African continent to the deltaic plain. The fluvial processes associated with the river have built the delta outward, creating a range of depositional environments from terrestrial to deep marine. As the delta has evolved, sediment supply has varied, influencing the size and nature of the deposits in different parts of the basin (Allen, 1970). The organic-rich shales of the Akata Formation, buried deep within the delta, were subjected to high temperatures and pressures over millions of years, converting the organic matter into hydrocarbons. These hydrocarbons then migrated upward through porous rock formations into the sandstones of the Agbada Formation, where they became trapped by impermeable shale layers. This process created the complex petroleum system of the Niger Delta, which includes source rocks, reservoir rocks, and trapping mechanisms (Olatunji, 2023). The Niger Delta is a world-class hydrocarbon province with complex geological and depositional features. Its lithology, dominated by the Benin, Agbada, and Akata Formations, represents a range of depositional environments from fluvial-deltaic to deep marine (Deigh, 2024). The ongoing tectonic activity, sediment supply, and subsidence have driven the evolution of the delta, making it a key region for oil and gas exploration.

Volume 2, Issue 3, 2026
https://doi.org/10.5281/zenodo.23624877

The wells located in the study area aim to tap into these hydrocarbon-rich formations, contributing to Nigeria's continued role as a major oil-producing nation delta (Spina et al., 2025).

II. THEORETICAL REVIEW

Well-log interpretation supports estimates of lithology, pore space, and fluid saturation that are useful for preliminary reservoir screening (Asquith et al., 2004). However, no single log-derived property uniquely predicts production. This section summarizes the definitions and equations used for the analysis, including their key assumptions and limitations. Total porosity (Φ) is the ratio of pore volume to bulk rock volume. It may be estimated using neutron and density responses where lithology, fluid and borehole effects are considered (Asquith et al., 2004).

$$\Phi = \frac{V_p}{V_t} \quad (1)$$

Where (Φ) = Porosity (fraction or percentage), (V_p) = Volume of pores (voids), (V_t) = Total volume of the rock

For density log-derived porosity (Φ_d)

$$\Phi_d = \frac{\rho_m - \rho_b}{\rho_m - \rho_f} \quad (2)$$

Where (ρ_m) = Matrix density (g/cc) (typically around 2.65 g/cc for sandstone), (ρ_b) = Bulk density from the log (g/cc), (ρ_f) = Fluid density (g/cc) (typically around 1.0 g/cc for water).

Water saturation (Sw) is the fraction of pore volume filled with water. Archie's relationship estimates Sw from resistivity in suitably clean formations, but conductive shale, variations in formation-water salinity and invasion can affect estimates (Sam-Marcus et al., 2018).

$$S_w^n = \frac{a \cdot R_w}{\phi^m \cdot R_t} \quad (3)$$

Where: (S_w) = Water saturation (fraction or percentage), (R_w) = Formation water resistivity (ohm-m), (R_t) = True resistivity of the formation (ohm-m) from the resistivity log, (ϕ) = Porosity (fraction), (a) = Tortuosity factor (typically assumed as 1), (m) = Cementation exponent (usually between 1.8 and 2), (n) = Saturation exponent (typically assumed as 2).

The Archie equation assumes a clean (non-shaly) formation. For shaly formations, corrections like the Simandoux or Dual Water models are often used to account for the additional conductivity due to the clay content (Ibrahim et al., 2022). The net-to-gross ratio is the fraction of the total interval that consists of reservoir-quality rock. It is a measure of the proportion of the zone that can effectively contribute to fluid flow (Egbele et al., 2005). This ratio is particularly useful in formations where the reservoir rock is interbedded with non-reservoir rock, such as shale.

$$\frac{\text{Net Thickness}}{\text{Gross Thickness}} = \frac{\text{Reservoir Quality Thickness}}{\text{Total Thickness of the Zone}} \quad (4)$$

Net-to-gross ratio (N/G) is dimensionless and typically ranges from 0 to 1. Higher values indicate better reservoir quality (Asquith et al., 2004).

The volume of clay is an important parameter, particularly in shaly formations, as it affects the reservoir's ability to store and transmit fluids. The Gamma Ray (GR) log is often used to estimate the volume of clay in the formation (El-Sawy et al., 2026).

$$V_{cl} = 0.33 \times \left(2^{3.7 \cdot \left(\frac{GR_{log} - GR_{min}}{GR_{max} - GR_{min}}\right)} - 1\right) \quad (5)$$

Where (GR_{log}) = Gamma Ray log reading in the zone of interest, (GR_{min}) = Minimum Gamma Ray reading (clean sand baseline), (GR_{max}) = Maximum Gamma Ray reading (shale baseline).

Volume 2, Issue 3, 2026
https://doi.org/10.5281/zenodo.23624877

Hydrocarbon-filled porosity-thickness ($\Phi S_o H$) is the product of porosity, hydrocarbon saturation and net thickness. It measures a pore-volume equivalent per unit area, not a full volumetric reserve estimate; conversion to hydrocarbons initially in place requires area, formation-volume factor and additional assumptions (Ahmed et al., 2019).

$\Phi, (S_o = 1 - S_w)$

$$\Phi S_o H = \Phi \cdot (1 - S_w) \quad (6)$$

Where Φ = porosity (fraction).(Φ), Sh = hydrocarbon saturation (fraction); Sh = 1 − Sw.(S_o), (H) = Net thickness (ft or m).

Hydrocarbon pore-volume provides an indication of the hydrocarbon storage capacity of a reservoir (El-Sawy et al., 2026). Porosity-thickness (ΦH) represents pore-space thickness per unit area. It is determined from representative net-interval porosity and net reservoir thickness. It does not independently describe fluid mobility or permeability (Anovitz & Cole, 2015).

$$\Phi H = \Phi \cdot H \quad (7)$$

Where (Φ) = Average porosity of the zone, (H) = Net thickness

This product is important for volumetric calculations and assessing the overall hydrocarbon potential of the reservoir. Water cut and oil cut are fractions of produced liquid rates. These production quantities are theoretical context only; neither was calculated because production-rate data were unavailable (Kamal et al., 2023).

$$WC = \frac{Q_w}{Q_o + Q_w} \quad (8)$$

Where (Q_w) = Water production rate, (Q_o) = Oil production rate

$$OC = 1 - WC \quad (9)$$

The resistivity index compares the resistivity of a hydrocarbon-bearing rock with that of an equivalent rock fully saturated with formation water (Jahanpanah & Tavakoli, 2026).

$$I_r = \frac{R_t}{R_0} \quad (10)$$

Where (R_t) = True formation resistivity, (R_0) = Formation resistivity when fully saturated with water.

This ratio is used to determine the hydrocarbon saturation when applied with Archie's equation. Together, gamma ray, resistivity, density, and neutron logs provide a basis for screening sand-prone units and estimating porosity and saturation.

III. MATERIALS AND METHODS

This study employed conventional well log datasets from two wells, hereafter referred to as Well 1 and Well 2, located within the Niger Delta Basin. The available datasets (Table 1) comprised well header information, well deviation data, and digital wireline logs. The well headers provided essential metadata, including well name, reference datum, total drilled depth, and spatial location. Deviation data, where available, contained measured depth, inclination, and azimuth information required for trajectory assessment and depth correction.

Table 1. Data Inventory of the Well Log Datasets used in this Study

Dataset / Log Type	Well 1	Well 2
Well header	Available	Available
Well deviation	Not available	Available
Gamma ray log	Available	Available

Volume 2, Issue 3, 2026
https://doi.org/10.5281/zenodo.23624877

Deep resistivity log	Available	Available
Bulk density log	Available	Available
Sonic log	Available	Available
Neutron porosity log	Available	Available

Petrophysical interpretation was performed using Interactive Petrophysics v3.4, a standard well log analysis software used for log editing, reservoir zonation, lithological interpretation, cross-plotting, and petrophysical parameter estimation. The input logs were supplied in ASCII format and included gamma ray, deep resistivity, bulk density, neutron porosity, and sonic logs. Log depths were recorded in feet, gamma ray values in API/GAPI, resistivity in ohm-m, bulk density in g/cm³, and neutron porosity in fractional units (Figure 3 and 4).

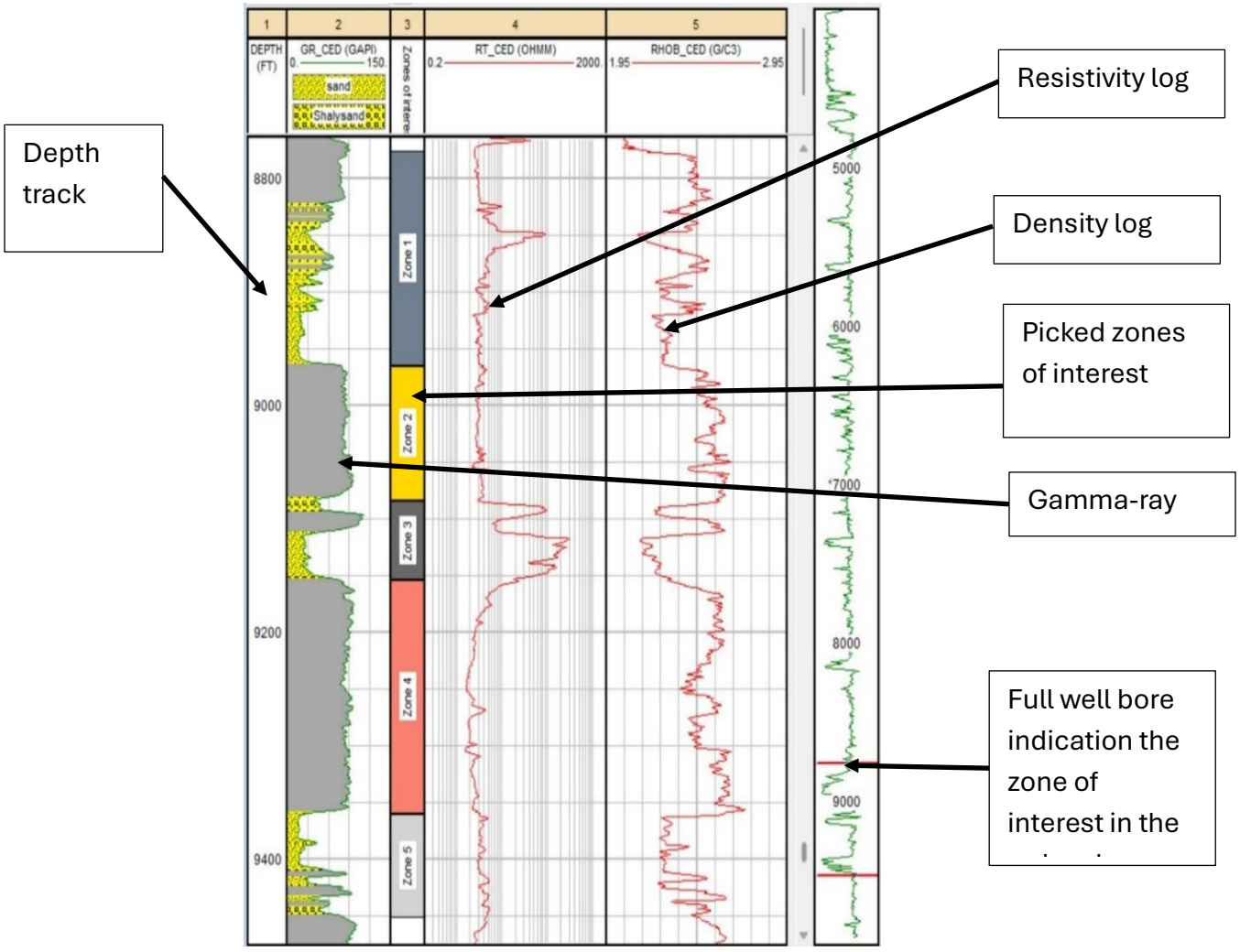


Figure 3: Input Logs for Well 1

Volume 2, Issue 3, 2026
https://doi.org/10.5281/zenodo.23624877

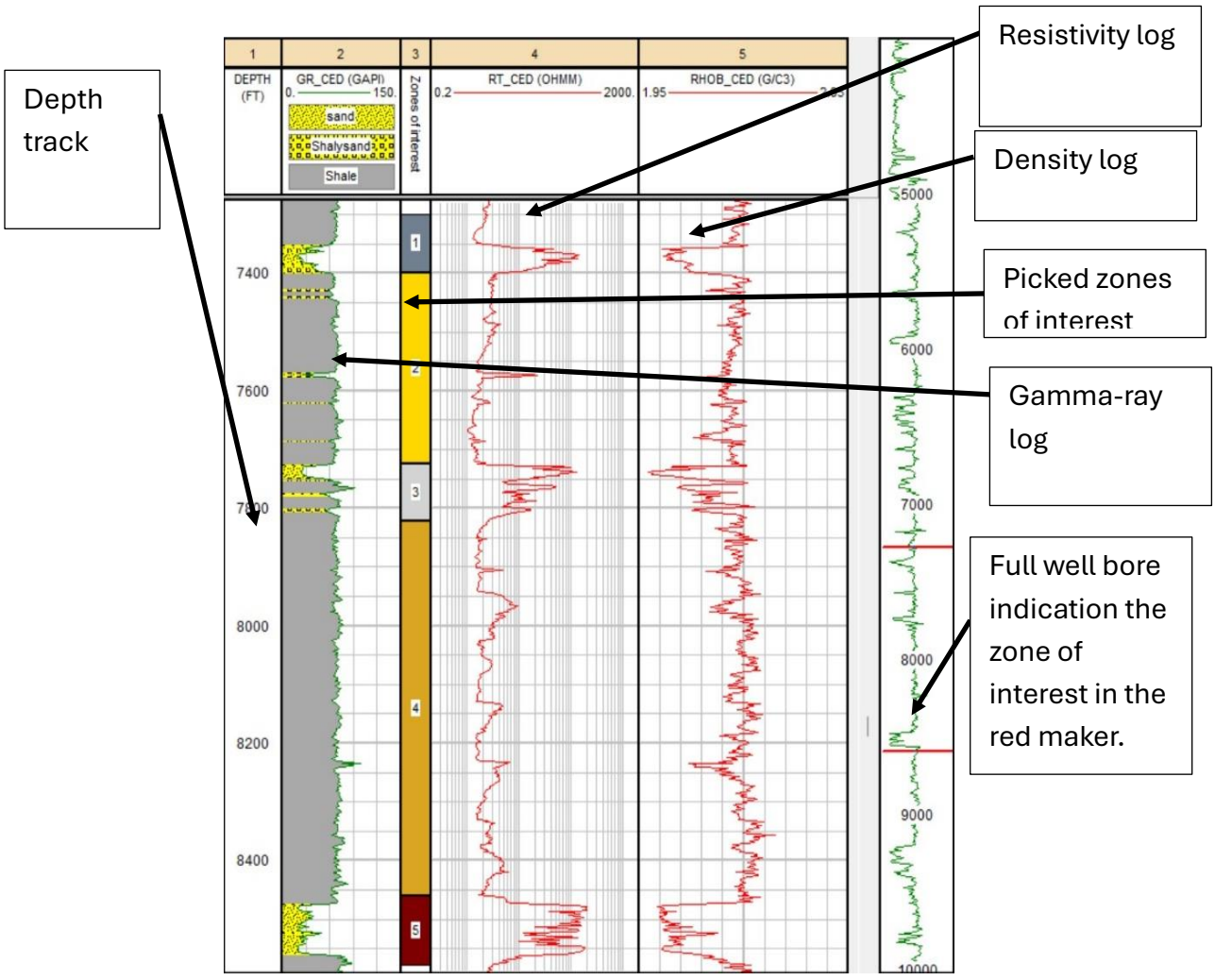


Figure 4: Input Logs for Well 2

The integrated log suite was used for reservoir identification, lithological discrimination, fluid typing, porosity estimation, shale volume calculation, water saturation estimation, net-to-gross evaluation, and thickness-weighted reservoir ranking.

Log Quality Control and Data Preparation

Prior to interpretation, the digital logs were imported into Interactive Petrophysics and inspected for completeness, depth consistency, curve availability, and anomalous readings. The log curves were checked visually to identify missing intervals, spurious spikes, unrealistic values, and depth mismatch between curves. Where necessary, minor log editing and curve conditioning were carried out to improve interpretability while preserving the original character of the dataset. The wells were analyzed using measured depth as the primary depth reference. For Well 2, where deviation data were available, the deviation survey supported the assessment of well trajectory and depth positioning. For Well 1, where deviation data were not available, interpretation was based on the

Volume 2, Issue 3, 2026
https://doi.org/10.5281/zenodo.23624877

supplied depth-referenced logs. All reservoir zones were identified consistently across the available log intervals using gamma ray, resistivity, density, and neutron responses.

Lithological Identification and Reservoir Zonation

Lithological identification and reservoir zonation were performed using integrated gamma-ray, resistivity, density, and neutron-porosity logs. Low gamma-ray responses indicated sand-dominated intervals, while high responses suggested shale-rich formations. Clean-sand and shale baselines were established at 22 and 90 API for Well 1 and 25 and 100 API for Well 2, respectively. Reservoir intervals were identified using minimum effective-porosity thresholds of approximately 10%, a maximum clay volume of 50%, and a maximum water saturation of 50%. Net-pay intervals were further constrained by a water-saturation cutoff of 34.6%, as summarized in Table 2b. reservoir zones were delineated in each well using integrated log responses. Gross thickness was determined from interval boundaries, while net reservoir thickness represented the cumulative thickness satisfying the applicable porosity, clay-volume, and water-saturation criteria. Net-to-gross ratio (N/G) was calculated as net reservoir thickness divided by gross thickness. Independent verification requires the original depth-based cutoff classifications.

Shale Volume Estimation

The volume of shale was estimated from the gamma ray log using the gamma ray index method. This approach normalizes the gamma ray response between the clean sand and shale baselines established for each well. The gamma ray index was calculated as:

$$\left[I_{GR} = \frac{GR_{log} - GR_{min}}{GR_{max} - GR_{min}}\right] \quad (11)$$

Here IGR is the gamma-ray index; GRlog is the recorded value and GRmin and GRmax are well-specific clean-sand and shale baselines, respectively. Values outside 0–1 are clipped for interpretation.

For this study, the gamma ray index was used as an approximation of shale volume:

$$[V_{sh} = I_{GR}] \quad (12)$$

Here Vsh is gamma-ray-derived shale volume, approximated by the linear gamma-ray index. This approximation may be affected by radioactive minerals and cannot distinguish clay types; calibration to other mineralogical information would be beneficial.

Porosity Estimation

Porosity was estimated using density and neutron porosity logs. The density-derived porosity was calculated from the bulk density log using:

$$\left[\phi_D = \frac{\rho_{ma} - \rho_b}{\rho_{ma} - \rho_f}\right] \quad (13)$$

Here ρma is assumed matrix density, ρb is bulk density and ρf is pore-fluid density. The original manuscript gives illustrative sandstone and water values (2.65 and 1.0 g/cm³), but does not specify which matrix and fluid values were actually applied in each interval.

The neutron porosity log provided an independent porosity estimate. To improve reliability, density and neutron porosity responses were compared across each reservoir interval. Where both curves showed consistent behaviour, an average effective porosity was computed as:

$$\left[\phi = \frac{\phi_D + \phi_N}{2}\right] \quad (14)$$

Volume 2, Issue 3, 2026
https://doi.org/10.5281/zenodo.23624877

Here Φavg is the displayed arithmetic neutron-density average, ΦD is density porosity and ΦN is neutron porosity. The original project settings, shale corrections and gas corrections were not supplied.

Fluid Identification and Hydrocarbon Discrimination

Fluid identification was performed by integrating deep resistivity, density, and neutron porosity responses. Intervals with low gamma ray, favourable porosity, and elevated deep resistivity were interpreted as potential hydrocarbon-bearing reservoirs. Water-bearing zones generally exhibit lower resistivity because formation water is conductive, whereas hydrocarbon-bearing intervals typically show higher resistivity due to the non-conductive nature of hydrocarbons. Neutron-density separation can be compatible with gas effects, but borehole conditions and lithological variation also cause separation. Without formation tests or fluid samples, resistivity and neutron-density responses identify only potentially hydrocarbon-bearing intervals and do not establish oil or gas unequivocally.

Water Saturation and Hydrocarbon Saturation Estimation

Water saturation was estimated using Archie's equation, which is commonly applied to clean sandstone reservoirs:

$$\left[S_w = \left(\frac{aR_w}{\phi^m R_t}\right)^{1/n}\right] \quad (15)$$

In Equation (15), a represents the tortuosity factor, Rw is formation-water resistivity (Ω·m), m is the cementation exponent, Rt is true formation resistivity (Ω·m), n is the saturation exponent, and Φ is effective porosity (fraction). Water saturation was estimated using Archie's equation in Interactive Petrophysics, with conventional parameters of a = 1, m = 1.8–2.0, and n = 2. The calculation depends on formation-water resistivity (Rw) and the selected model parameters.

Hydrocarbon saturation was then calculated as:

$$[S_h = 1 - S_w] \quad (16)$$

For oil-bearing intervals, oil saturation was expressed as:

$$[S_o = 1 - S_w] \quad (17)$$

Equations (16)–(17) define complementary pore-fluid saturation. In the absence of an independent fluid-type test, the reported values should be called hydrocarbon saturation (Sh) rather than unqualified oil saturation. Interval-average saturation values were used for the tabulated screening indicators.(S_o).

Net-to-Gross Ratio Estimation

The net-to-gross ratio was calculated to evaluate the proportion of reservoir-quality sand within each gross reservoir interval. Net thickness was defined as the cumulative thickness of clean, porous, and potentially hydrocarbon-bearing sand. Gross thickness was defined as the total thickness between the top and base of each reservoir zone.

The net-to-gross ratio was calculated as:

$$\left[N/G = \frac{H_{net}}{H_{gross}}\right] \quad (18)$$

Here Hnet is the cumulative interpreted net reservoir thickness and Hgross is the depth difference between top and base. Ratios are dimensionless. Although the reported N/G calculations can be checked, reproducing net thickness requires the original explicit cutoffs and interval flags.

Volume 2, Issue 3, 2026
https://doi.org/10.5281/zenodo.23624877

Thickness-Weighted Reservoir Quality Metrics

Thickness weighting was applied as a comparison of established volumetric screening indicators, not as a new petrophysical model. Two metrics were calculated for each zone: porosity-thickness ($\phi \cdot H$) and hydrocarbon-filled porosity-thickness ($\phi S_h \cdot H$), both in feet because thickness is reported in feet.

Porosity–thickness was calculated as:

$$[\phi \cdot H = \phi \times H_{net}] \quad (19)$$

$\phi \cdot H$ is the product of zone-average porosity (fraction) and reported net thickness (ft). It indicates an equivalent net pore-space thickness, not absolute pore volume or flow capacity.

Oil-filled porosity–thickness was calculated as:

$$[\phi S_o \cdot H = \phi \times S_o \times H_{net}] \quad (20)$$

$\phi S_h \cdot H$ equals zone-average porosity multiplied by the complement of zone-average water saturation and by net thickness. It is an approximate hydrocarbon-filled thickness indicator. Using products of interval averages differs from a sample-by-sample integral if porosity and saturation covary; that uncertainty cannot be tested without the underlying curves. Each metric was recalculated from the displayed rounded averages as an internal arithmetic check. Differences of a few hundredths of a foot are attributable to tabular rounding; a full audit requires the unrounded Interactive Petrophysics exports. The metrics were used to screen relative storage potential, without claiming validation against permeability, pressure, well tests or production.

Reservoir and Net-Pay Cutoff Determination

Reservoir and net-pay intervals were evaluated using petrophysical cutoff criteria based on effective porosity (PHIE), water saturation (Sw), and clay volume (Vcl). Net reservoir intervals were defined by minimum effective-porosity thresholds, a maximum clay volume of 50%, and a maximum water saturation of 50%. Net-pay intervals were further restricted by a stricter water-saturation cutoff of 34.6%. The minimum effective-porosity cutoff was generally 10%, with zone-specific thresholds of 10.1% for Zone 1 and 25.8% for Zone 3. No minimum bed-thickness restriction was imposed. Gross thickness was calculated from reservoir top and bottom depths, while net reservoir and net-pay thicknesses were determined by summing depth increments satisfying their respective cutoff criteria. Net-to-gross ratio (N/G) was calculated as net reservoir thickness divided by gross thickness. The cutoff criteria are summarized in Table 2.

Table 2. Petrophysical cutoff criteria reported for Wells 1 and 2

Parameter	Net reservoir cutoff	Net-pay cutoff
Effective porosity (PHIE)	≥10%; Zone 1: ≥10.1%; Zone 3: ≥25.8%	Same zone-specific thresholds
Water saturation (Sw)	≤50%	≤34.6%
Clay volume (Vcl)	≤50%	≤50%
Minimum bed thickness	0 m	0 m

Reservoir Ranking Workflow

Reservoir ranking followed five stages: (i) interpret lithology and gross intervals from integrated logs; (ii) estimate porosity; (iii) derive water saturation from the assumed Archie model; (iv) record interpreted net thickness and calculate N/G; and (v) compare ΦH and $\phi S_h \cdot H$ alongside saturation

Volume 2, Issue 3, 2026
https://doi.org/10.5281/zenodo.23624877

and shale volume. The ranking is descriptive rather than statistically validated, given the small two-well dataset and absence of performance outcomes.

Higher $\phi \cdot H$ and $\phi S_h \cdot H$ imply greater interpreted pore-space and hydrocarbon-filled thickness per unit area, not necessarily greater deliverability. Zones with very limited net thickness were classified as lower-priority appraisal targets rather than categorically non-producible.

IV. RESULTS AND DISCUSSION

A. Lithostratigraphic Correlation

Figure 4 presents a preliminary lithostratigraphic comparison of the two wells. Similar gamma-ray patterns suggest possible correlative units, but the correlation does not confirm continuous fluid-connected reservoirs without structural interpretation, seismic ties and pressure evidence. Five reservoir zones were identified across the wells based on the integrated interpretation of gamma ray, resistivity, density, and neutron porosity logs. These zones were further evaluated using conventional petrophysical parameters and thickness-weighted metrics to determine their reservoir quality and hydrocarbon potential.

B. Petrophysical Evaluation of Well 1

The petrophysical results for Well 1 are presented in Table 3 and Figure 5. Five reservoir zones were identified between 8776 ft and 9452 ft. The zones were evaluated using gross thickness, net thickness, net-to-gross ratio, average porosity, average water saturation, average clay volume, porosity–thickness $(\phi \cdot H)$, oil-filled porosity–thickness $(\phi S_o \cdot H)$, and clay-volume–thickness $(V_{cl} \cdot H)$.

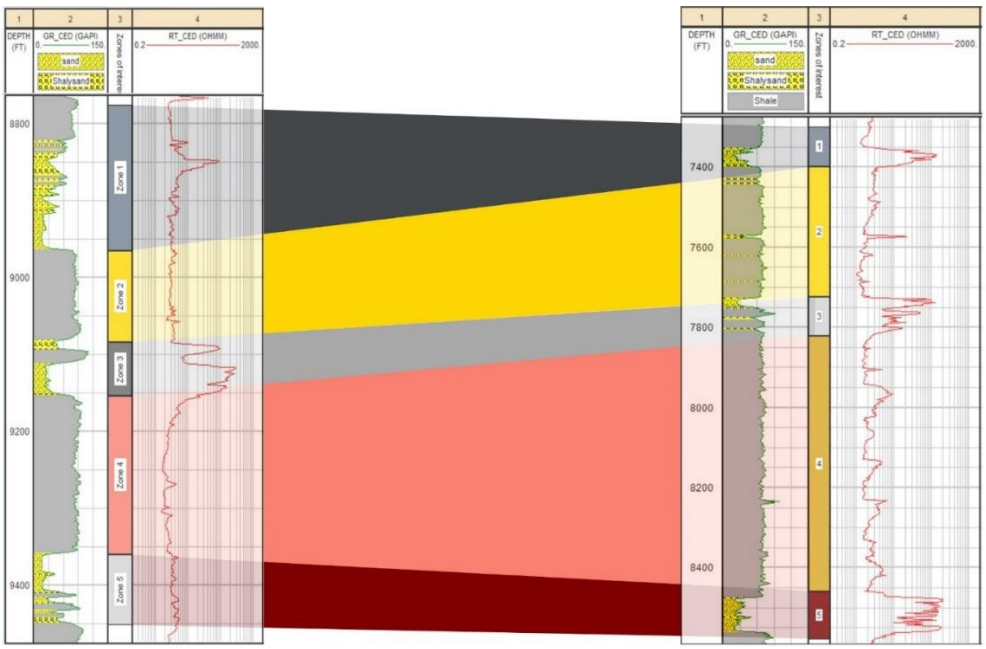


Figure. 5. Correlation Panel showing the Typical Subsurface Bedding and Lithostratigraphic Continuity across the Study Area

Volume 2, Issue 3, 2026
https://doi.org/10.5281/zenodo.23624877

Table 3. Petrophysical Results for Well 1

Well	Zone Name	Units	Top	Bottom	Gross	Net	N/G	Av Phi	Av Sw	Av Vcl	$\phi \cdot H$	$\phi S_o \cdot H$	$V_{cl} \cdot H$
01	Zone 1	ft	8776	8965	189	108.5	0.574	0.248	0.289	0.201	26.87	19.09	21.8
01	Zone 2	ft	8965	9084	119	2	0.017	0.18	0.465	0.082	0.36	0.19	0.16
01	Zone 3	ft	9084	9154	70	52	0.743	0.269	0.068	0.126	13.99	13.04	6.58
01	Zone 4	ft	9154	9360	206	0.5	0.002	0.167	0.466	0.044	0.08	0.04	0.02
01	Zone 5	ft	9360	9452	92	59.5	0.647	0.268	0.281	0.126	15.93	11.45	7.51

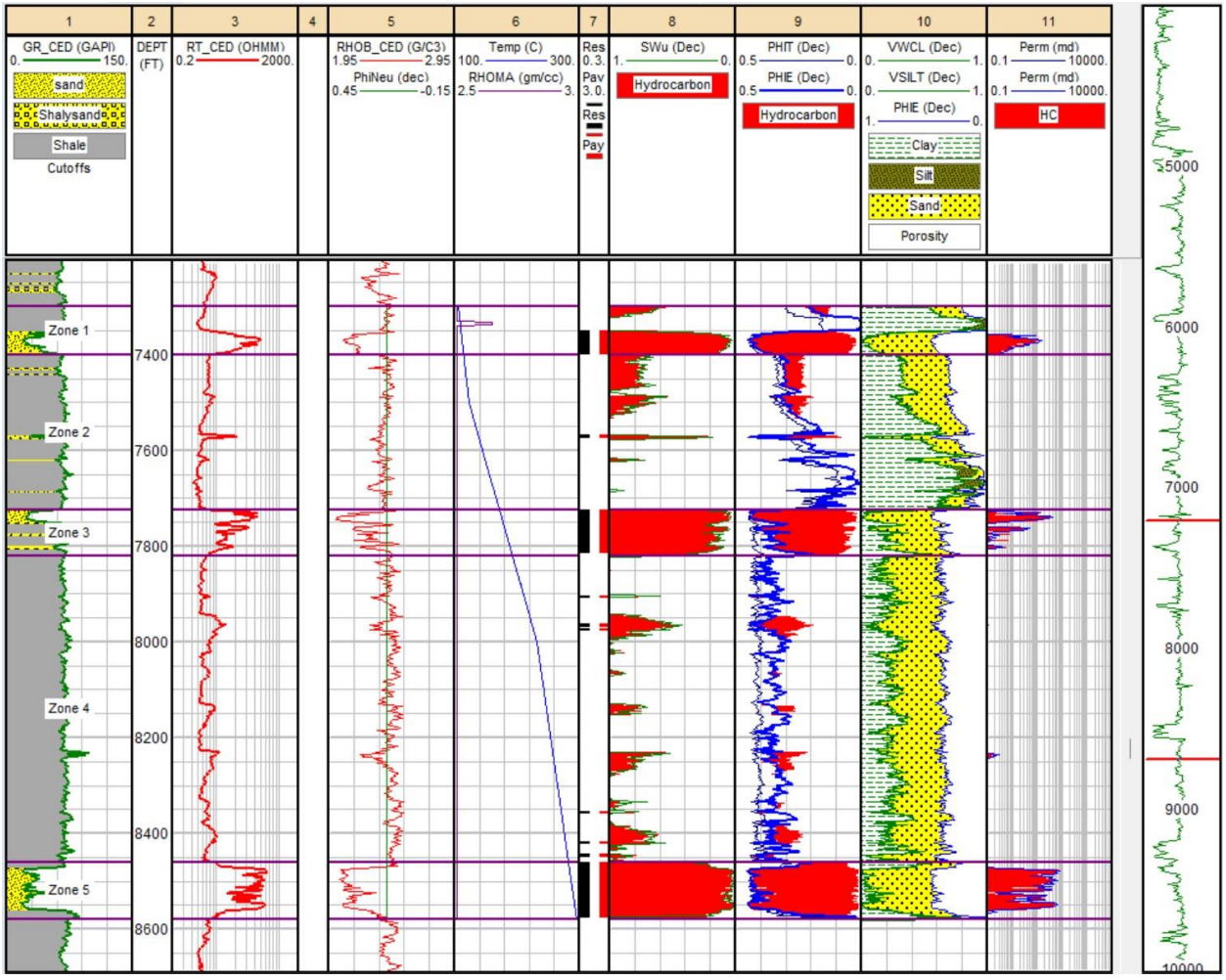


Figure 6. Petrophysical Interpretation Results for Well 1.

Zone 1: 8776–8965 ft

Zone 1 has a gross thickness of 189 ft and a net thickness of 108.5 ft, giving a net-to-gross ratio of 0.574. This indicates that more than half of the interval consists of reservoir-quality sand. The average porosity is 24.8%, suggesting good storage capacity, while the average water saturation of 28.9% indicates moderate hydrocarbon saturation. The average clay volume of 20.1% suggests some shale influence, which may affect permeability. However, the high value of 26.87 and value of 19.09 support favourable interpreted pore-space and hydrocarbon-filled thickness.

Volume 2, Issue 3, 2026
https://doi.org/10.5281/zenodo.23624877

Zone 2: 8965–9084 ft
Zone 2 has a gross thickness of 119 ft but only 2 ft of net reservoir thickness, resulting in a very low net-to-gross ratio of 0.017. Although the average porosity is 18.0%, the high water saturation of 46.5% and very low net thickness significantly reduce its reservoir potential. The values are 0.36 and 0.19, respectively, indicating negligible hydrocarbon storage capacity. This zone is therefore interpreted as low-priority for further appraisal based on these logs alone.

Zone 3: 9084–9154 ft
Zone 3 displays favourable reservoir characteristics, with a net-to-gross ratio of 0.743 and a net thickness of 52 ft within a gross interval of 70 ft. The average porosity is 26.9%, while the water saturation is very low at 6.8%, indicating high hydrocarbon saturation. The average clay volume of 12.6% is relatively moderate and does not significantly reduce the reservoir quality. The value of 13.99 and value of 13.04 support a favourable log-derived hydrocarbon-filled thickness. Zone 3 is therefore one of the most prospective intervals in Well 1.

Zone 4: 9154–9360 ft
Zone 4 has the poorest reservoir quality in Well 1. Although the gross interval is 206 ft thick, the net reservoir thickness is only 0.5 ft, giving an extremely low net-to-gross ratio of 0.002. The average porosity is 16.7%, and the water saturation is high at 46.6%. The very low and values of 0.08 and 0.04, respectively, indicate negligible reservoir storage and hydrocarbon capacity. This interval is therefore classified as a low-priority interval for further appraisal.

Zone 5: 9360–9452 ft
Zone 5 shows good reservoir potential, with a gross thickness of 92 ft and a net thickness of 59.5 ft, corresponding to a net-to-gross ratio of 0.647. The average porosity is 26.8%, indicating good pore-volume capacity. The average water saturation of 28.1% suggests moderate hydrocarbon saturation, while the average clay volume of 12.6% indicates relatively clean reservoir conditions. The value of 15.93 and value of 11.45 support the interpretation of Zone 5 as a potentially hydrocarbon-bearing reservoir interval. Zones 1, 3, and 5 represent the most favourable reservoir intervals in Well 1. Zones 2 and 4 show poor reservoir potential due to low net thickness, low net-to-gross ratios, and high-water saturation.

Petrophysical Evaluation of Well 2

The petrophysical results for Well 2 are presented in Table 4 and Figure 7. Five reservoir zones were identified between 7300 ft and 8580 ft. Compared with Well 1, Well 2 generally shows high porosity values and stronger thickness-weighted hydrocarbon indicators, particularly in Zones 3 and 5.

Table 4. Petrophysical Results for Well 2

Well	Zone Name	Units	Top	Bottom	Gross	Net	N/G	Av Phi	Av Sw	Av Vcl	$\phi \cdot H$	$\phi S_o \cdot H$	$V_{cl} \cdot H$
02	Zone 1	ft	7300	7400	100	48	0.48	0.403	0.1	0.105	19.34	17.4	5.03
02	Zone 2	ft	7400	7723.5	323.5	6	0.019	0.418	0.253	0.07	2.51	1.88	0.42
02	Zone 3	ft	7723.5	7821.5	98	91.5	0.934	0.367	0.122	0.184	33.62	29.51	16.8
02	Zone 4	ft	7821.5	8459.5	638	6.25	0.01	0.429	0.445	0.047	2.68	1.49	0.29
02	Zone 5	ft	8459.5	8580	120.5	111.25	0.923	0.394	0.055	0.125	43.81	41.39	13.9

Volume 2, Issue 3, 2026
https://doi.org/10.5281/zenodo.23624877

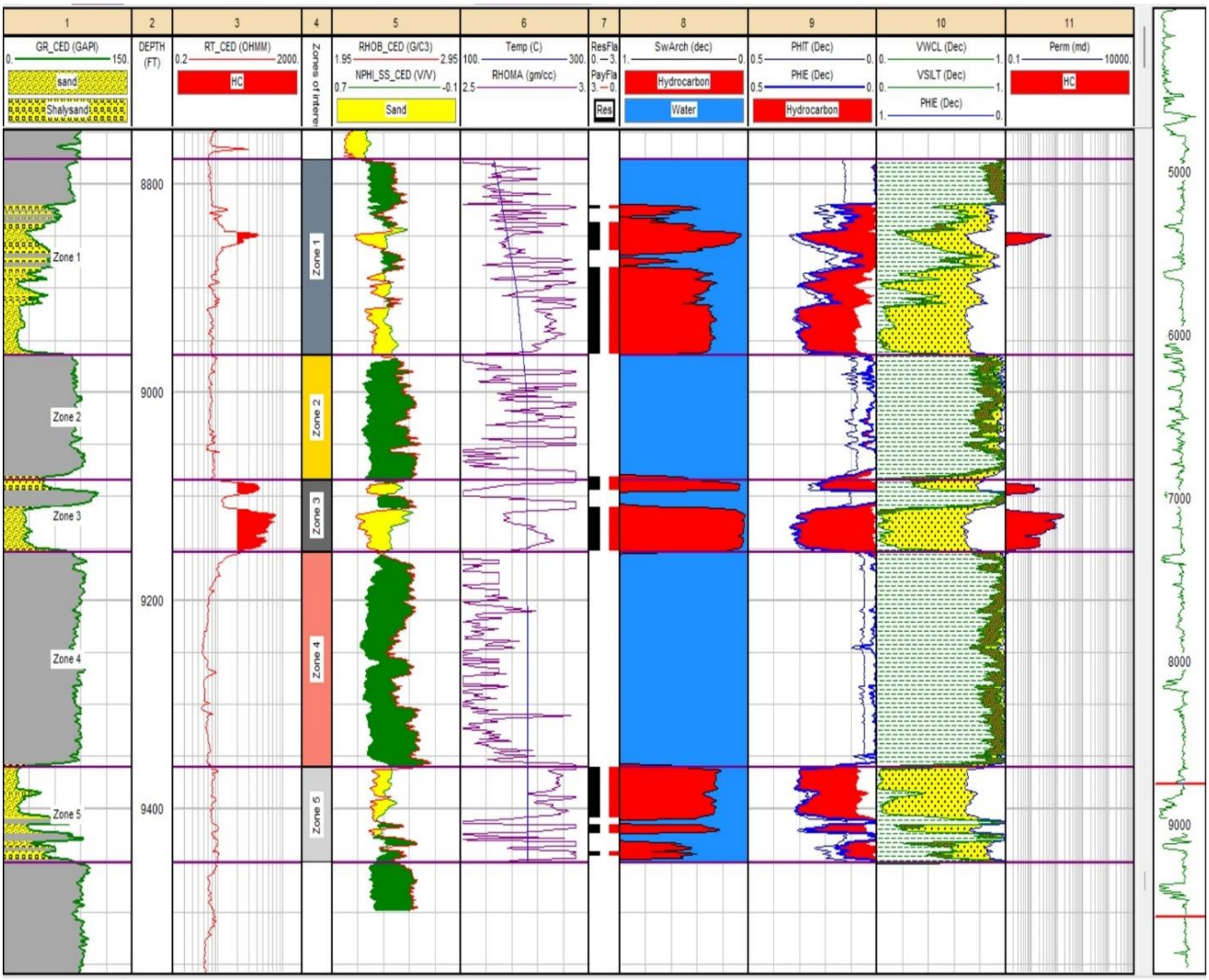


Figure 7. Petrophysical Interpretation Results for Well 2.

Zone 1: 7300–7400 ft

Zone 1 has a gross thickness of 100 ft and a net thickness of 48 ft, resulting in a net-to-gross ratio of 0.480. The average porosity is high at 40.3%, suggesting excellent pore-volume capacity. The low water saturation of 10.0% indicates strong hydrocarbon saturation, while the clay volume of 10.5% suggests relatively clean reservoir conditions. The values of 19.34 and 17.40, respectively, indicate favourable log-derived hydrocarbon-filled thickness.

Zone 2: 7400–7723.5 ft

Zone 2 has a gross thickness of 323.5 ft but a net thickness of only 6 ft, giving a net-to-gross ratio of 0.019. Although the average porosity is high at 41.8%, the very limited net thickness substantially reduces its reservoir significance. The average water saturation of 25.3% is moderate, but the low $(\phi \cdot H)$ and $(\phi S_o \cdot H)$ values of 2.51 and 1.88, respectively, indicate limited hydrocarbon-bearing capacity. This zone is therefore considered to have poor reservoir potential.

Volume 2, Issue 3, 2026
https://doi.org/10.5281/zenodo.23624877

Zone 3: 7723.5–7821.5 ft
Zone 3 is one of the best reservoir intervals in Well 2. It has a gross thickness of 98 ft and a net thickness of 91.5 ft, producing a very high net-to-gross ratio of 0.934. The average porosity is 36.7%, indicating excellent storage capacity, while the low water saturation of 12.2% suggests strong hydrocarbon saturation. Although the clay volume is 18.4%, the high net thickness and high porosity compensate for the shale content. The value of 33.62 and value of 29.51 indicate favourable interpreted hydrocarbon-filled thickness for Zone 3.

Zone 4: 7821.5–8459.5 ft
Zone 4 spans 638 ft gross but contains only 6.25 ft of interpreted net reservoir, giving N/G = 0.010. Its reported average porosity is high (42.9%), not low; however, water saturation is also relatively high (44.5%) and the net interval is very thin. Consequently, ΦH = 2.68 ft and ΦShH = 1.49 ft, which place this zone among the lower-priority screening targets. High porosity in isolation does not compensate for extremely limited net reservoir thickness.

Zone 5: 8459.5–8580 ft
Zone 5 is the most prospective interval in Well 2. It has a gross thickness of 120.5 ft and a net thickness of 111.25 ft, giving a high net-to-gross ratio of 0.923. The average porosity is 39.4%, indicating excellent reservoir storage capacity, while the very low water saturation of 5.5% indicates strong hydrocarbon saturation. The average clay volume of 12.5% suggests manageable shale content. The values of 43.81 and 41.39, respectively, are the highest among all evaluated zones, making Zone 5 the highest-ranked log-derived hydrocarbon-filled thickness interval in the study.

Figure 8 shows that Well 1 Zones 1, 3 and 5 have larger net-to-gross ratios than Zones 2 and 4. Zone 1 has the largest reported hydrocarbon-filled porosity-thickness in Well 1 (19.09 ft), although Zone 3 has lower water saturation (6.8%). Zones 2 and 4 are low-priority targets principally because of their small net thicknesses, not because porosity or saturation alone determines productivity.

Volume 2, Issue 3, 2026
https://doi.org/10.5281/zenodo.23624877

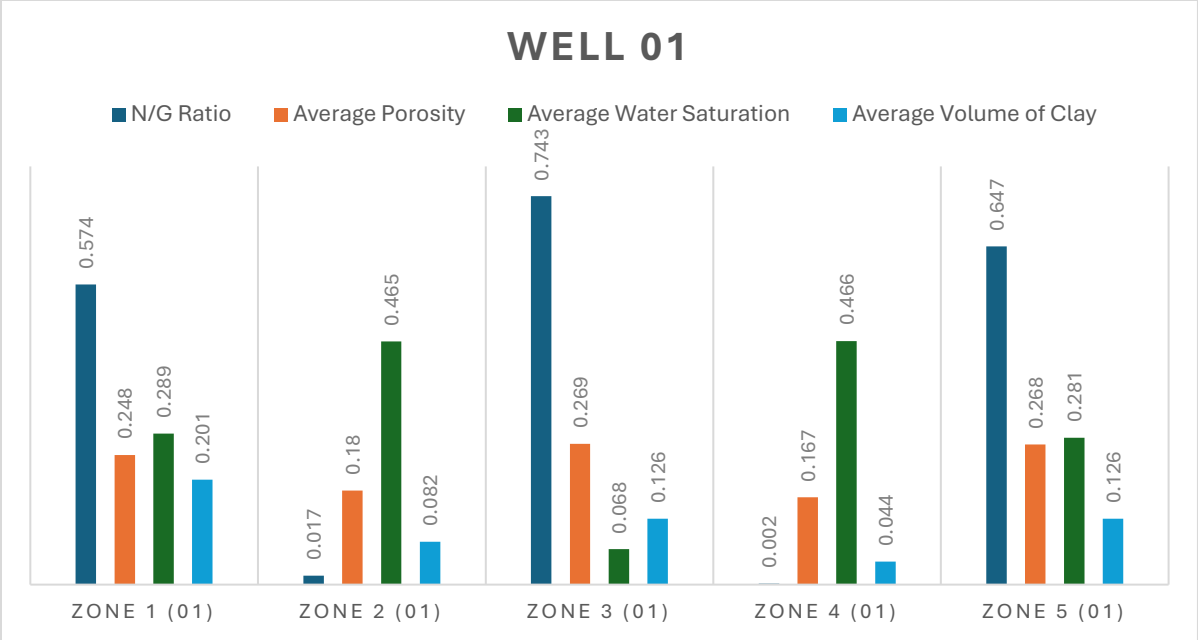


Figure 8: Bar chart showing Petrophysical results across all 5 Zone for well 1

Figure 9 shows that Well 2 Zones 3 and 5 combine high N/G (0.934 and 0.923), high average porosity (36.7% and 39.4%), and LOW water saturation (12.2% and 5.5%). In contrast, Zone 4 has HIGH porosity (42.9%) but low N/G (0.010) and relatively high water saturation (44.5%). Zone 2 likewise has high porosity (41.8%) yet only 6 ft of interpreted net reservoir thickness. These findings correct the previously contradictory descriptions of high saturation in Zones 3 and 5 and low porosity in Zone 4.

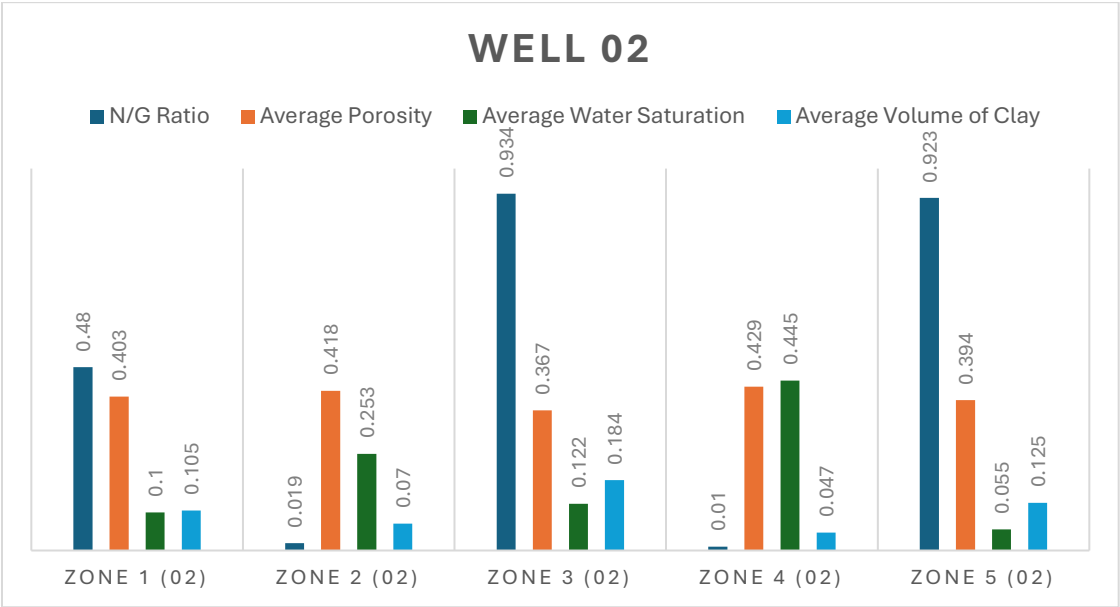


Figure 9: Bar chart showing Petrophysical results across all 5 Zone for well 2

Volume 2, Issue 3, 2026
https://doi.org/10.5281/zenodo.23624877

Comparative Reservoir Ranking

The comparative evaluation of both wells shows that reservoir quality is controlled not only by porosity but also by net thickness, water saturation, and net-to-gross ratio. In Well 1, Zones 1, 3, and 5 exhibit the best reservoir characteristics, with Zone 1 having the highest $(\phi \cdot H)$ and $(\phi S_o \cdot H)$ values. Zone 3, although thinner than Zone 1, has very low water saturation and a high net-to-gross ratio, making it highly prospective. Zone 5 also shows good hydrocarbon potential due to its favourable porosity, net thickness, and moderate water saturation. In Well 2, Zones 3 and 5 clearly dominate the reservoir ranking. Zone 5 has the highest $(\phi \cdot H)$ and $(\phi S_o \cdot H)$ values in the entire study, indicating the greatest hydrocarbon-bearing storage capacity. Zone 3 also shows excellent reservoir quality due to its high net-to-gross ratio, high net thickness, and low water saturation. Zone 1 is also prospective, although its net-to-gross ratio and thickness-weighted values are lower than those of Zones 3 and 5. Zones 2 and 4 in both wells are consistently poor reservoir intervals. Although some of these zones display moderate to high porosity, their very low net-to-gross ratios and limited net thickness result in weak $(\phi \cdot H)$ and $(\phi S_o \cdot H)$ values. This demonstrates that porosity alone is not sufficient for reservoir evaluation. A zone may have high porosity but still possess poor reservoir potential if the effective net thickness is small or if water saturation is high.

Discussion of Thickness-Weighted Metrics

Conventional porosity and water saturation represent interval-average rock and fluid properties; by themselves they do not account for the amount of qualifying reservoir rock. The established $\phi \cdot H$ and $\phi S_o \cdot H$ products incorporate net thickness and hence change the screening order in intervals with high porosity but low net thickness. This is a comparison of ranking behaviour rather than proof of greater predictive accuracy: there are no core permeability, pressure, production or well-test measurements against which to test reliability. The distinction is illustrated by Well 2: Zone 4 has the highest reported average porosity (42.9%) but its $\phi S_o \cdot H$ is only 1.49 ft because net thickness is 6.25 ft and water saturation is 44.5%. Zone 5 has lower porosity (39.4%) but a much larger $\phi S_o \cdot H$ (41.39 ft), supported by 111.25 ft of net thickness and 5.5% water saturation. This contrast provides direct numerical support for the usefulness of thickness weighting as a screening measure, without implying it predicts production. The strongest hydrocarbon potential is observed in Well 2, particularly in Zones 3 and 5. These zones combine high porosity, high net-to-gross ratio, low water saturation, and large net thickness. In contrast, well 1 shows more moderate reservoir development, with Zones 1, 3, and 5 representing the main prospective intervals. The results therefore suggest that Well 2 contains better-developed reservoir sands and stronger hydrocarbon-bearing capacity than Well 1. The two-well comparison supports thickness-integrated screening of potentially hydrocarbon-bearing intervals.

V. CONCLUSION

This study assessed ten gross evaluation zones across two Niger Delta wells using conventional logs and the established thickness-weighted screening indicators $\phi \cdot H$ and $\phi S_o \cdot H$. The comparison demonstrates how interpreted net reservoir thickness, porosity and water saturation jointly influence relative storage indicators; the analysis does not independently establish fluid type, producibility or recoverable reserves. In Well 1, Zones 1, 3, and 5 represent the main prospective intervals. Zone 1 recorded the highest pore-volume indicator in the well, with a net thickness of 108.5 ft, net-to-gross ratio of 0.574, average porosity of 24.8%, water saturation of

Volume 2, Issue 3, 2026
https://doi.org/10.5281/zenodo.23624877

28.9%, $(\phi \cdot H)$ of 26.87 ft, and $(\phi S_o \cdot H)$ of 19.09 ft. Zone 3 also showed strong reservoir quality, with the highest net-to-gross ratio in Well 1 at 0.743, average porosity of 26.9%, very low water saturation of 6.8%, and $(\phi S_o \cdot H)$ of 13.04 ft. Zone 5 recorded a net-to-gross ratio of 0.647, average porosity of 26.8%, and $(\phi S_o \cdot H)$of 11.45 ft. In contrast, Zones 2 and 4 are poor reservoir intervals, with net-to-gross ratios of only 0.017 and 0.002, and very low $(\phi S_o \cdot H)$ values of 0.19 ft and 0.04 ft, respectively. In Well 2, Zones 3 and 5 are the highest-ranked potentially hydrocarbon-bearing intervals. Zone 5 is the highest-ranked zone in the entire study, with a net thickness of 111.25 ft, net-to-gross ratio of 0.923, average porosity of 39.4%, very low water saturation of 5.5%, of 43.81 ft, and of 41.39 ft. Zone 3 also shows excellent reservoir potential, with a net thickness of 91.5 ft, net-to-gross ratio of 0.934, average porosity of 36.7%, water saturation of 12.2%, of 33.62 ft, and of 29.51 ft. Zone 1 is also favourable, with average porosity of 40.3%, water saturation of 10.0%, and of 17.40 ft. Zones 2 and 4 are less prospective because their net-to-gross ratios are very low, at 0.019 and 0.010, despite having high porosity values above 41%. Across the two wells, Well 2 Zone 5 has the largest reported $\phi S_o \cdot H$ (41.39 ft), compared with 19.09 ft for Well 1 Zone 1. These figures indicate more than twice the hydrocarbon-filled pore-space thickness per unit area in the former interval under the source assumptions, not twice the recoverable reserves or production rate. High-porosity Well 2 Zones 2 and 4 (41.8% and 42.9%) illustrate the importance of accounting for their small net thicknesses and low N/G. On the reported $\phi S_o \cdot H$ values, the six leading intervals are Well 2 Zone 5 (41.39 ft), Well 2 Zone 3 (29.51 ft), Well 1 Zone 1 (19.09 ft), Well 2 Zone 1 (17.40 ft), Well 1 Zone 3 (13.04 ft), and Well 1 Zone 5 (11.45 ft). These represent priorities for additional appraisal, subject to verification of the original model inputs, cutoff criteria and fluid interpretation. The value of thickness-weighted metrics lies in comparative screening, not demonstrated superiority in predicting reservoir productivity.

DECLARATIONS

Consent for Publication

All authors have read and approved the final version of the manuscript titled “Integrated Petrophysical Evaluation of Reservoir Quality and Hydrocarbon Potential Using Thickness-Weighted Metrics from Well Logs in the Niger Delta” and consent to its publication. The authors confirm that the manuscript does not contain any individual person’s data, images, or personal clinical information requiring additional consent for publication.

Competing Interests

The authors declare that they have no competing financial or non-financial interests that could have influenced the work reported in this manuscript.

Funding

This research did not receive any specific grant from funding agencies in the public, commercial, or not-for-profit sectors. The work was conducted as part of independent academic research activities of the authors.

Availability of Data and Materials

The well log dataset used in this study was acquired from Frandee Consulting Services, Yenagoa, through authorized academic access. The data are not publicly available due to access and confidentiality restrictions. However, derived datasets generated during the present study,

including processed well logs, interpreted reservoir zones, petrophysical results, tables, Figures, and images, are available from the corresponding author upon reasonable request.

Authors' Contributions

Dr. Francis Omonefe, conducted the petrophysical data processing and quantitative analysis, performed reservoir zonation, calculated the thickness-weighted metrics, interpreted the well log results, prepared the Figures and tables, and drafted the original manuscript.

Dr. Edeye Ejaita conceptualized the study, acquired the well log dataset, contributed to the geological and petrophysical interpretation, supported the structural and reservoir analysis, and reviewed and revised the manuscript.

Arekumo ThankGod assisted with data validation, software implementation, quality control of the well log interpretation, and verification of the petrophysical modelling outputs.

All authors reviewed, edited, and approved the final version of the manuscript.

ACKNOWLEDGMENTS

The authors acknowledge Frandee Consulting Services, Yenagoa, for providing access to the well log dataset used in this study through authorized academic access. The authors also appreciate the Departments of Geology and Physics at Federal University Otuoke and Niger Delta University for their academic support and enabling environment during the preparation of this research. The authors are grateful to all individuals and institutions whose support contributed to the successful completion of this study.

REFERENCES

Ahmed, S., Elwegaa, K., Htawish, M., & Alhaj, H. (2019). Determination of the oil initial in place, reserves, and production performance of the Safsaf C oil reservoir. *The International Journal of Engineering and Science, 8*(2), 86–97. https://doi.org/10.9790/1813-0802018697

Allen, J. R. L. (1970). Sediments of the modern Niger Delta: A summary and review. In J. P. Morgan (Ed.), *Deltaic sedimentation, modern and ancient* (SEPM Special Publication No. 15, pp. 138–151). Society of Economic Paleontologists and Mineralogists. https://doi.org/10.2110/pec.70.11.0138

Anovitz, L. M., & Cole, D. R. (2015). Characterization and analysis of porosity and pore structures. *Reviews in Mineralogy and Geochemistry, 80*(1), 61–164. https://doi.org/10.2138/rmg.2015.80.04

Arochukwu, E., Ugwueze, C., & Udom, G. (2023). Depositional facies analysis of coastal to shallow marine deposits in the onshore Niger Delta Basin: Accessing the influence of sedimentology and depositional environments on reservoir quality. *Scientia Africana, 22*(1), 335–354. https://doi.org/10.4314/sa.v22i1.28

Asquith, G., Krygowski, D., Henderson, S., & Hurley, N. (2004). Porosity logs. In *Basic well log analysis* (pp. 37–76). American Association of Petroleum Geologists. https://doi.org/10.1306/mth16823c4

Bassey, D. K. (2015). *Application of dielectric logging tool in formation evaluation*. https://www.academia.edu/16629374/APPLICATION_OF_DIELECTRIC_LOGGING_TOOL_IN_FORMATION_EVALUATION

Bello, A., Jamaludin, S. N. F., Babikir, I. A. M., Mohammed, H. S., & Salman, N. F. I. (2026). Integrated geological and petrophysical assessment of caprock integrity and reservoir in FX Field, Central Luconia, Sarawak. *Geological Journal*. https://doi.org/10.1002/gj.70195

Bonne, K. P. M. (2014). Reconstruction of the evolution of the Niger River and implications for sediment supply to the Equatorial Atlantic margin of Africa during the Cretaceous and the Cenozoic. *Geological Society, London, Special Publications, 386*(1), 327–349. https://doi.org/10.1144/SP386.20

Chukwuemeka, E. V., Ogbamikhumi, A., Salami, S. A., & Didi, C. N. (2025). Structural evaluation and hydrocarbon potentials of Emil Field, offshore Niger Delta Basin. *Results in Earth Sciences, 3*, 100142. https://doi.org/10.1016/j.rines.2025.100142

Deabl, R., Ramadhan, A., & Al-Dabaj, A. (2021). Evaluation of petrophysical properties interpretations from log interpretation for Tertiary reservoir/Ajeel Field. *Iraqi Journal of Oil and Gas Researches, 1*(1), 28–44. https://doi.org/10.55699/ijogr.2021.0101.1009

Deigh, C. (2024). Integrated reservoir characterization of deepwater turbidite systems: A systematic review of seismic attribute analysis, well log integration, and dynamic data validation, with a focus on the Niger Delta Fold Belt. *International Journal of Multidisciplinary Research and Growth Evaluation, 5*(6), 1798–1814. https://doi.org/10.54660/.ijmrge.2024.5.6.1798-1814

Doust, H., & Omatsola, E. (1989). Niger Delta. In *Divergent/passive margin basins*. American Association of Petroleum Geologists. https://doi.org/10.1306/M48508C4

Egbele, E., Ezuka, I., & Onyekonwu, M. (2005). Net-to-gross ratios: Implications in integrated reservoir management studies. In *Nigeria Annual International Conference and Exhibition*. Society of Petroleum Engineers. https://doi.org/10.2118/98808-MS

Ejaita, E., & Omonefe, F. (2026). Multi-attribute predictions of volume of shale and porosity from seismic data over Akaso Field, Niger Delta using machine learning regression analysis. *Discover Geoscience, 4*(1). https://doi.org/10.1007/s44288-026-00457-x

El-Sawy, M. Z., Nabawy, B. S., Shazly, T. F., & Saleh, A. H. (2026). Assessing the unconventional reservoirs of the Nukhul Formation in the Rudeis-Sidri Field, Gulf of Suez: Petrophysical characterization and flow unit discrimination. *Scientific Reports, 16*(1). https://doi.org/10.1038/s41598-026-49085-y

Ezeh, S. C., Mode, W. A., Adejinmi, K., & Ozumba, B. M. (2016). Ichnological characteristics and variability of Miocene deposits in the Cenozoic Niger Delta: Examples from cores in the Coastal Swamp and Offshore depobelts. *Palaeogeography, Palaeoclimatology, Palaeoecology, 454*, 189–201. https://doi.org/10.1016/j.palaeo.2016.04.043

Haack, R. C., Sundararaman, P., Diedjomahor, J. O., Xiao, H., Gant, N. J., May, E. D., & Kelsch, K. (2000). Niger Delta petroleum systems, Nigeria. In *Petroleum systems of South Atlantic margins* (pp. 213–231). American Association of Petroleum Geologists. https://doi.org/10.1306/M73705C16

Herlinger, R. (2019). Dielectric logging: Principles, applications, and examples from the Brazilian oilfields. In *Offshore Technology Conference Brasil*. https://doi.org/10.4043/29882-MS

Huang, Y., Yu, X., & Fu, C. (2025). Depositional architecture of aggrading delta front distributary channels and corresponding depositional evolution process in Ordos Basin: Implications for deltaic reservoir prediction. *Water, 17*(4), 528. https://doi.org/10.3390/w17040528

Ibrahim, A. F., Elkatatny, S., & Ramadan, M. A. (2022). Prediction of water saturation in tight gas sandstone formation using artificial intelligence. *ACS Omega, 7*(1), 215–222. https://doi.org/10.1021/acsomega.1c04416

Jahanpanah, A., & Tavakoli, V. (2026). Pore type pathways to hydrocarbon potential: Electrical resistivity in Permian–Triassic Persian Gulf carbonates. *Journal of Petroleum Exploration and Production Technology, 16*(2). https://doi.org/10.1007/s13202-026-02130-y

Kamal, B., Abbasi, Z., & Hassanzadeh, H. (2023). Water-cut measurement techniques in oil production and processing—A review. *Energies, 16*(17), 6410. https://doi.org/10.3390/en16176410

Kiss, T., Gönczy, S., Nagy, T., Mesaroš, M., & Balla, A. (2022). Deposition and mobilization of microplastics in a low-energy fluvial environment from a geomorphological perspective. *Applied Sciences, 12*(9), 4367. https://doi.org/10.3390/app12094367

Knackstedt, M., Carnerup, A., Golab, A., Sok, R., Young, B., & Riepe, L. (2013). Petrophysical characterization of unconventional reservoir core at multiple scales. *Petrophysics, 54*(3), 216–223.

Konyukhov, A. I. (2008). Sedimentary basins of passive margins filled with sediments of river deltas and submarine fans. *Lithology and Mineral Resources, 43*(6), 507–519. https://doi.org/10.1134/S0024490208060011

Kuye, D. A., & Hampson, G. J. (2023). Sedimentological and tectono-stratigraphic characterisation of a shallow-marine reservoir, 'Dona' Field, offshore Niger Delta. *Marine and Petroleum Geology, 158*, 106517. https://doi.org/10.1016/j.marpetgeo.2023.106517

Momta, P. S., Omoboh, J. O., & Odigi, M. I. (2015). Sedimentology and depositional environment of D2 sand in part of Greater Ughelli Depobelt, onshore Niger Delta, Nigeria. *American Journal of Engineering and Applied Sciences, 8*(4), 556–566. https://doi.org/10.3844/ajeassp.2015.556.566

Nabawy, B. S. (2025). New approaches in reservoir characterization utilizing conventional and special core analyses: A comprehensive review. *Journal of Umm Al-Qura University for Applied Sciences*. https://doi.org/10.1007/s43994-025-00225-6

Nikolaev, M., & Kazak, A. (2019). Liquid saturation evaluation in organic-rich unconventional reservoirs: A comprehensive review. *Earth-Science Reviews, 194*, 327–349. https://doi.org/10.1016/j.earscirev.2019.05.012

Olabode, S. O. (2006). Siliciclastic slope deposits from the Cretaceous Abeokuta Group, Dahomey (Benin) Basin, southwestern Nigeria. *Journal of African Earth Sciences, 46*(3), 187–200. https://doi.org/10.1016/j.jafrearsci.2006.04.008

Olabode, S. O., & Mohammed, M. Z. (2016). Depositional facies and sequence stratigraphic study in parts of Benin (Dahomey) Basin, southwestern Nigeria: Implications for the reinterpretation of Tertiary sedimentary successions. *International Journal of Geosciences, 7*(2), 210–228. https://doi.org/10.4236/ijg.2016.72017

Olatunji, O. A. (2023). Palynofacies and sedimentology of HB-001 well. *Malaysian Journal of Geosciences, 7*(2), 79–86. https://doi.org/10.26480/mjg.02.2023.79.86

Omoja, U., Egwuonwu, G. N., Omonefe, F., & Okeugo, C. (2026). Reservoir quality assessment using petrophysical analysis in Uzondu Field, Niger Delta Basin. https://jirbdai.com.ng/index.php/jirbdai/article/view/297

Omonefe, F., Ejaita, E., & Rowland, E. D. (2020). Lithological investigation at Tombia and Opolo using vertical electrical soundings and pseudo tomogram. *International Journal of Latest Technology in Engineering, Management & Applied Science*.

Osman, M., Farouk, S., & Sarhan, M. A. (2025). Integrated 3D reservoir modelling for unconventional reservoir prospects: A case study of Upper Cretaceous Brown Limestone reservoir, South Geisum Field, Gulf of Suez, Egypt. *Geomechanics and Geophysics for Geo-Energy and Geo-Resources, 11*(1). https://doi.org/10.1007/s40948-024-00919-x

Overare, B., Azmy, K., Garzanti, E., Avwenagha, E. O., & Emudianughe, J. E. (2024). Diagenetic imprints in the reservoirs of Agbada Formation, Niger Delta Basin: Implication for reservoir quality and appraisal of calcite cement. *Marine and Petroleum Geology, 163*, 106746. https://doi.org/10.1016/j.marpetgeo.2024.106746

Plumley, L. P. S. W. J., V. (1992). A model for sandstone compaction by grain interpenetration. *Journal of Sedimentary Research, 62*. https://doi.org/10.1306/D4267875-2B26-11D7-8648000102C1865D

Reijers, T. (2011). Stratigraphy and sedimentology of the Niger Delta. *Geologos, 17*(3). https://doi.org/10.2478/v10118-011-0008-3

Reijers, T., Petters, S., & Nwajide, C. (1997). The Niger Delta Basin. In *Sedimentary basins of the world* (pp. 151–172). https://doi.org/10.1016/S1874-5997(97)80010-X

Sam-Marcus, J., Enaworu, E., Rotimi, O. J., & Seteyeobot, I. (2018). A proposed solution to the determination of water saturation: Using a modelled equation. *Journal of Petroleum Exploration and Production Technology, 8*(4), 1009–1015. https://doi.org/10.1007/s13202-018-0453-4

Sarhan, M. A. (2025). Unconventional hydrocarbon resources of Egypt. *Discover Geoscience, 3*(1). https://doi.org/10.1007/s44288-025-00235-1

Senosy, A. H., Ewida, H. F., Soliman, H. A., & Ebraheem, M. O. (2020). Petrophysical analysis of well logs data for identification and characterization of the main reservoir of Al Baraka Oil Field, Komombo Basin, Upper Egypt. *SN Applied Sciences, 2*(7). https://doi.org/10.1007/s42452-020-3100-x

Shabani, M., Yarmohammadi, S., & Ghaffary, S. (2022). Reservoir quality investigation by combination of core measured data and NMR technique analysis: A case study of Asmari carbonate reservoir in Gachsaran Field. *Carbonates and Evaporites, 38*(1). https://doi.org/10.1007/s13146-022-00824-y

Sharif, F. (2024). *Reservoir evaluation techniques: Combining data interpretation and geological analysis for accurate hydrocarbon assessment and petrophysical properties*. https://www.researchgate.net/publication/384919775_Reservoir_Evaluation_Techniques_Combining_Data_Interpretation_and_Geological_Analysis_for_Accurate_Hydrocarbon_Assessment_and_Petrophysical_Properties

Sneider, R., Tinker, C., & Meckel, L. (1978). Deltaic environment reservoir types and their characteristics. *Journal of Petroleum Technology, 30*(11), 1538–1546. https://doi.org/10.2118/6701-PA

Spina, V., Soto, J. I., Ringenbach, J., & Mazzoli, S. (2025). Shale tectonics in the hyperextended continental margin of the Niger Delta. *Tectonics, 44*(7). https://doi.org/10.1029/2024TC008689

Stoneley, R. (1966). The Niger Delta region in the light of the theory of continental drift. *Geological Magazine, 103*(5), 385–397. https://doi.org/10.1017/S0016756800053978

Volokitin, Y., & Khabarov, A. (2010). Interactive petrophysical model of oilfields with large transition zones: Salym Fields example. In *SPE Russian Oil and Gas Conference and Exhibition*. Society of Petroleum Engineers. https://doi.org/10.2118/138093-MS

Zhang, Z., Zhang, H., Li, J., & Cai, Z. (2020). Permeability and porosity prediction using logging data in a heterogeneous dolomite reservoir: An integrated approach. *Journal of Natural Gas Science and Engineering, 86*, 103743. https://doi.org/10.1016/j.jngse.2020.103743